

The influence of cyclic loading histories on soil-geogrid interface behaviour under pullout conditions

Marilene Pisano, Giuseppe Cardile & Nicola Moraci
Mediterranea University of Reggio Calabria, DICEAM, Italy

ABSTRACT: The knowledge of soil-geosynthetic interaction is a key point in the design of geosynthetic reinforced soil structures. With regard to the pullout limit state, pullout tests can simulate it by using large-scale laboratory apparatus, and they allow studying the interaction mechanisms that develop in the anchorage zone. During the service life of geosynthetic-reinforced soil structures, geogrids may be subjected to cyclic or dynamic loads in addition to the sustained tensile load acting under service load conditions. In order to define the peak pullout resistance mobilized after a cyclic loading history (a sinusoidal load with fixed amplitude A , number of cycles N and frequency f) and to analyse the cyclic strain behaviour of soil-geosynthetic interface, the writers carried out a series of multi-stage pullout tests on an HDPE extruded uniaxial geogrid embedded in a well-compacted granular soil for different vertical effective stress σ'_v values. The test results show that the design pullout resistance parameters could be affected by the applied cyclic history for specific combined loading conditions (A , N and σ'_v) and it should be taken into account for designing geosynthetic reinforced soil structures.

Keywords: geosynthetics, geogrid, pullout, multi-stage testing, monotonic, cyclic, soil-geogrid interface, multi-stage test, design parameters

1 INTRODUCTION

Modelling the soil-geosynthetic interface is extremely important in order to better design geosynthetic-reinforced soil (GRS) structures by means of numerical methods. For this purpose, it is necessary to analyse the soil-geosynthetic interaction in terms of pullout resistance and strain behaviour under both monotonic and cyclic loading conditions. Several researches have studied these aspects (Yasuda *et al.* 1992; Min *et al.* 1995; Raju and Fannin 1997; Nernheim 2005; Moraci and Cardile 2009; Nayeri and Fakharian 2009; Moraci and Cardile 2012), but the investigated frequencies were too low to be representative of long-term vehicular loads or short-term seismic loads. In this context, the paper aims to investigate the pullout behaviour of an HDPE geogrid embedded in a well-compacted granular soil, subject to cyclic pullout loading with a higher frequency ($f = 1$ Hz), varying the tensile load amplitude and the effective vertical stress.

2 EXPERIMENTAL STUDY

2.1 Apparatus

The test apparatus (Moraci and Recalcati 2006; Cardile *et al.* 2016a) comprises a large pullout steel box (1700x600x680 mm), a vertical load application system (PVC bag filled with air), a hydraulic actuator system for displacement- or load-controlled testing, a special clamp assembly, a pair of sleeves, and all the required instrumentation (load cell, LVDT).

2.2 Test materials

The soil used in this research is an uniform medium sand classified as SP and A-3 according to USCS and CNR-UNI 10006 classification systems respectively, with grain shape ranging from sub-rounded to rounded, uniformity coefficient ($U=D_{60}/D_{10}$) equal to 1.96, and average grain size (D_{50}) equal to 0.32 mm. Standard Proctor compaction tests gave a maximum dry unit weight $\gamma_{dmax}=16.24$ kN/m³ at an optimum water content $w_{opt}=13.5\%$. Direct shear tests, performed at 95% of γ_{dmax} , yielded values of the peak shear-strength angle ϕ'_p from 48° (for $\sigma'_v=10$ kPa) to 42° (for $\sigma'_v=100$ kPa). The shear-strength angle at constant volume ϕ'_{CV} was equal to 34° (Moraci and Recalcatti 2006).

The geosynthetic used in pullout tests is an HDPE uniaxial extruded geogrid. Its mechanical behaviour was investigated by means of wide-width tensile tests (Cardile *et al.* 2016b; Cardile *et al.* 2017b) in the standard atmosphere for testing (20±2°C at 65+5% RH) at constant strain rate equal to 20% per minute, using index test procedures (ISO 10319:2015). Additional monotonic tensile tests at constant strain rate equal to $\epsilon'=0.2\%$ per minute were also carried out to make comparison with the rate used in monotonic pullout tests. Table 1 lists the monotonic tensile test results at constant strain rates equal to 20% and 0.2% per minute.

Table 1. Wide-width tensile test results of the geogrid used in this research.

$T_{max} (\epsilon'=20\%/min)$ [kN/m]	$\epsilon_{max} (\epsilon'=20\%/min)$ [kN/m]	$J_{sec2\%} (\epsilon'=20\%/min)$ [kN/m]	$T_{max} (\epsilon'=0.2\%/min)$ [kN/m]	$\epsilon_{max} (\epsilon'=0.2\%/min)$ [kN/m]	$J_{sec2\%} (\epsilon'=0.2\%/min)$ [kN/m]
Maximum tensile strength per unit width	Tensile strain for $T_{max} (\epsilon'=20\%/min)$	Secant tensile stiffness at 2% strain	Maximum tensile strength per unit width	Tensile strain for $T_{max} (\epsilon'=0.2\%/min)$	Secant tensile stiffness at 2% strain
159	12.2	2454	103.5	14.5	1525

2.3 Test procedure

The multi-stage pullout tests were carried out on geogrid specimens 1.15 m long, at different vertical effective stresses ($\sigma'_v=10, 25, 50, 100$ kPa), by using a multi-stage procedure (MS) consisting of three steps (Moraci and Cardile 2009, 2012):

- a monotonic stage at constant rate of displacement (CRD) equal to 1 mm per minute, reaching a fixed pullout load P_i chosen as a percentage of P_R , that is the peak pullout resistance (per unit width) obtained by monotonic pullout tests at the same confining pressure and CRD=1 mm per min;
- a load-controlled cyclic stage using a sinusoidal function, with a fixed tensile loading amplitude A (chosen as a percentage of P_R) and frequency $f=1$ Hz, for 1000 cycles in total;
- a post-cyclic stage at CRD=1 mm per minute until pullout or specimen rupture occurs.

Table 2 lists the MS pullout test program, highlighting that the actually-made cycles were lower than the planned ones for the higher applied amplitude ($A\cong 45\% P_R$) at $\sigma'_v < 100$ kPa due to the pullout failure.

Table 2. MS pullout test program.

Test	N (planned)	N (actually-made)	σ'_v [kPa]	P_i [kN/m]	A [kN/m]
01	1000	1000	10	$\cong 35\% P_R$ (10 kPa)	$\cong 30\% P_R$ (10 kPa)
02	1000	20	10	$\cong 35\% P_R$ (10 kPa)	$\cong 45\% P_R$ (10 kPa)
03	1000	1000	25	$\cong 35\% P_R$ (25 kPa)	$\cong 30\% P_R$ (25 kPa)
04	1000	148	25	$\cong 35\% P_R$ (25 kPa)	$\cong 45\% P_R$ (25 kPa)
05	1000	1000	50	$\cong 35\% P_R$ (50 kPa)	$\cong 30\% P_R$ (50 kPa)
06	1000	158	50	$\cong 35\% P_R$ (50 kPa)	$\cong 45\% P_R$ (50 kPa)
07	1000	1000	100	$\cong 35\% P_R$ (100 kPa)	$\cong 30\% P_R$ (100 kPa)
08	1000	1000	100	$\cong 35\% P_R$ (100 kPa)	$\cong 45\% P_R$ (100 kPa)

3 ANALYSIS OF TEST RESULTS

The parameters obtained for each unload–reload cycle are (figure 1):

- Cyclic displacement's increment measured at the first confined section of specimen (the specimen head attached to the clamp) reached during each cyclic loading, $\Delta\delta_{part,i}^h$;
- Cumulative cyclic displacement of the specimen's first confined section, $\Delta\delta_i^h = \sum_{i=1}^N \Delta\delta_{part,i}^h$;
- Cyclic displacement's increment measured at the rear end of the specimen (the last transverse rib) reached during each cyclic loading, $\Delta\delta_{part,i}^e$;
- Cumulative cyclic displacement of the specimen's rear end, $\Delta\delta_i^e = \sum_{i=1}^N \Delta\delta_{part,i}^e$.

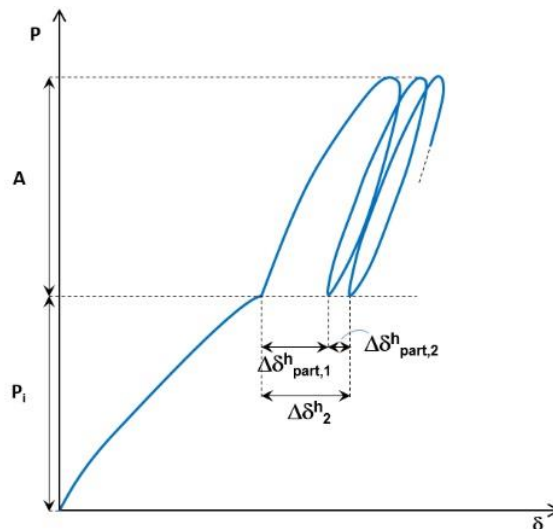


Figure 1. Schematic representation of different parameters obtained during hysteresis loops in multi-stage tests

For each of these parameters, the influence of tensile loading amplitude A , number of cycles N and vertical effective stress σ'_v was investigated.

In order to analyse the behaviour at the soil-reinforcement interface, the conceptual model proposed by Raju and Fannin, 1997 was modified by using a double-graph that shows the relationship between the number of cycles N and $\Delta\delta^h$ in the left part, and between $\Delta\delta^e$ and $\Delta\delta^h$ in the right one. These graphic representations (Figures 2 and 3) allow understanding when the behaviour of soil-reinforcement interface is stable/unstable. Specifically, it is stable when:

- The curve in the left graph is concave upward and $\Delta\delta^h$ becomes constant with increasing numbers of cycles;
- The curve in the right graph evolves inside the admissible area with cyclic displacement's increments of the specimen's first confined section that are higher than the correspondent cyclic displacement's increment of the specimen's rear end for all cycles.

Vice versa, the soil-geogrid interface behaviour is unstable when:

- The curve in the left graph has an inflection point becoming concave downward, and $\Delta\delta^h$ continues to increase with increasing numbers of cycles;
- The curve in the right graph becomes parallel at the boundary line between admissible and inadmissible area (the displacement's increment of geogrid's head is equal to the displacement's increment measured at the rear end for all the next cycles).

Nevertheless, it is important to observe that even a concave upward curve could be unacceptable if the cumulative displacements during the cyclic stage are larger than the allowable displacement for the serviceability limit state.

With regard to the influence of loading amplitude A , Figure 2a,b shows the results of MS pullout tests at equal values of $\sigma'_v=50$ kPa and $P_i\cong 35\% P_R$, performed with two different loading amplitudes ($A\cong 30\% P_R$; $A\cong 45\% P_R$).

In Figure 2a, when $A\cong 30\% P_R$ it is possible to observe a stable behaviour of soil-reinforcement interface during all the cyclic stage since $\Delta\delta^h$ tends to settle towards a constant value with increasing numbers of cycles. Same conclusions can be made looking at the Figure 2b, as for all cycles the cyclic displacement's increment measured at the rear end is lower than the cyclic displacement's increment of the geogrid's head. Referring to the results obtained with $A\cong 45\% P_R$ (Figure 2a), an unstable behaviour can be observed since there is an inflection point, and $\Delta\delta^h$ continues to increase with increasing numbers of cycles. The unstable behaviour arises even in the right graph (Figure 2b) as the $\Delta\delta^e-\Delta\delta^h$ curve becomes par-

allel to the boundary line between admissible and inadmissible area, which represents the pullout condition ($\Delta\delta_{part}^e = \Delta\delta_{part}^h$). Therefore, it is clear that the stability of soil-geogrid interface starts getting worse with increasing cyclic loading amplitude.

To evaluate the influence of the vertical effective stress σ'_v applied to the soil-geogrid interface, the strain behaviour has been investigated analysing MS pullout tests carried out with loading amplitude $A \approx 45\% P_R$ (the MS pullout tests at $A \approx 30\% P_R$ are omitted as they showed a stable behaviour for all the vertical effective stresses applied). Looking at the Figure 3a,b the only stable behaviour is obtained for $\sigma'_v = 100$ kPa. For all the other vertical effective stresses applied, the cumulative cyclic displacement of the specimen's head keeps on increasing until the clamp reaches the end.

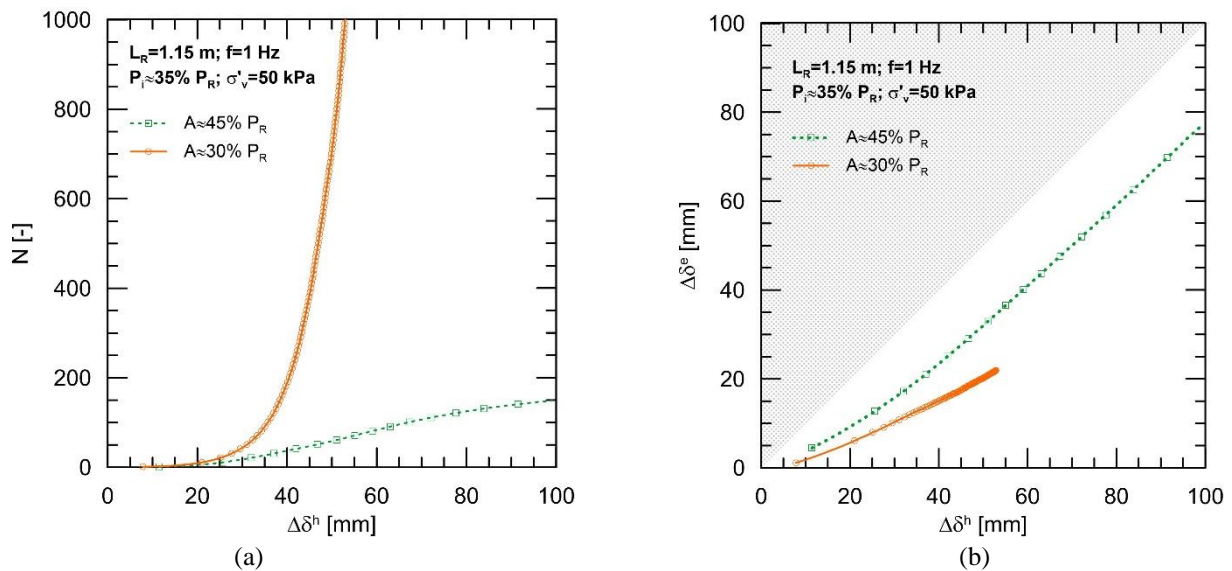


Figure 2. Number of loading cycles versus cumulative cyclic displacement measured at the first confined section of specimen (a), and $\Delta\delta_{part}^e$ versus cumulative cyclic displacement measured at the rear end of the specimen (b) for loading amplitudes $A \approx 30\% P_R$ and $45\% P_R$ and $\sigma'_v = 50$ kPa.

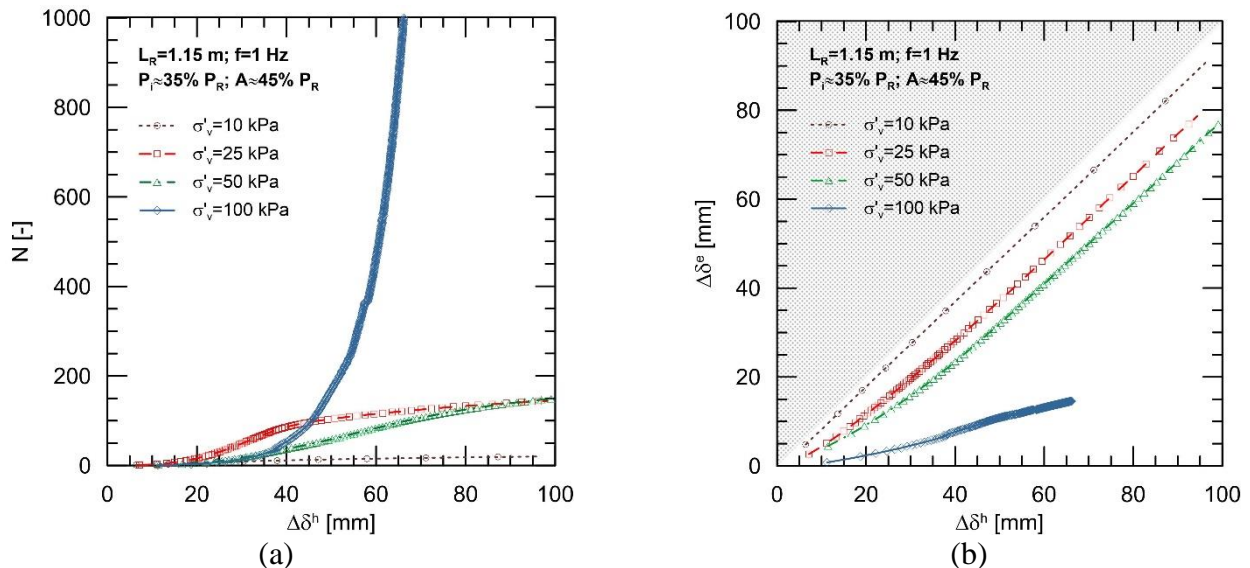


Figure 3. Number of loading cycles versus cumulative cyclic displacement of the specimen's first confined section (a) and $\Delta\delta^e$ versus cumulative cyclic displacement of the specimen's rear end (b) for varying vertical effective stress at loading amplitude $A \approx 45\% P_R$.

Figure 3b shows the relationship between the cumulative cyclic displacements of the specimen's first confined section, $\Delta\delta^h$, and the cumulative cyclic displacements of the specimen's rear end, $\Delta\delta^e$. The unstable behaviour can be observed for $\sigma'_v = 10, 25$ and 50 kPa since their representative curves become parallel to the boundary line between admissible and inadmissible area. Therefore, it is possible to observe that the increasing of the vertical effective stress σ'_v plays a stabilising role.

The influence of cyclic loading history on the peak pullout resistance has also been investigated by comparing the pullout curves for the MS tests and those for the corresponding CRD monotonic tests. The comparison is reported in figure 4a for the MS pullout test with $A \approx 30\% P_R$ and $\sigma'_v = 25$ kPa; this test is qualitatively representative of all those performed. Figure 4b illustrates the post-cyclic peak pullout re-

sistance P_R^{PC} normalised with respect to P_R , obtained in all MS tests with $A \approx 30\% P_R$ for varying vertical effective stresses. These results suggest that cyclic loading histories induce a reduction in peak pullout resistance with decreasing vertical effective stresses. For these specific test conditions, the post-cyclic peak pullout resistance reaches decreases up to 27% compared to the values that are obtained in monotonic pullout tests at the same test conditions (figure 4b). The higher decrease was measured at the lower σ'_v investigated, while post-cyclic pullout resistance remains almost equal to the corresponding monotonic value at the higher σ'_v .

Some observations can be made about the reduction of the interface design parameters in post-cyclic conditions. The first one is that in the third phase of MS tests the cumulative displacement of each transversal bar is higher than the cumulative displacement mobilised at the same pullout load level in the corresponding monotonic test. In view of the fact that the soil shear-strength angle depends on the shear displacement and considering the progressive failure mechanism developed by means of the elementary interaction mechanisms at the interface (Dyer 1985; Bergado *et al.* 1993; Ziegler and Timmers 2004; Palmeira 2009; Zhou *et al.* 2012; Calvarano *et al.* 2014; Jacobs *et al.* 2014; Cardile *et al.* 2017a; Moraci *et al.* 2017), an important reduction of the resistance's reserve occurs. The second observation concerns the higher decreasing of post-cyclic pullout resistance at the lower vertical effective stresses: it could be due to the soil dilatancy effect (the difference between peak and residual resistance values increases with decreasing vertical effective stress), entailing it that the cumulative displacements along the geogrid are higher than those measured at the higher vertical stresses investigated.

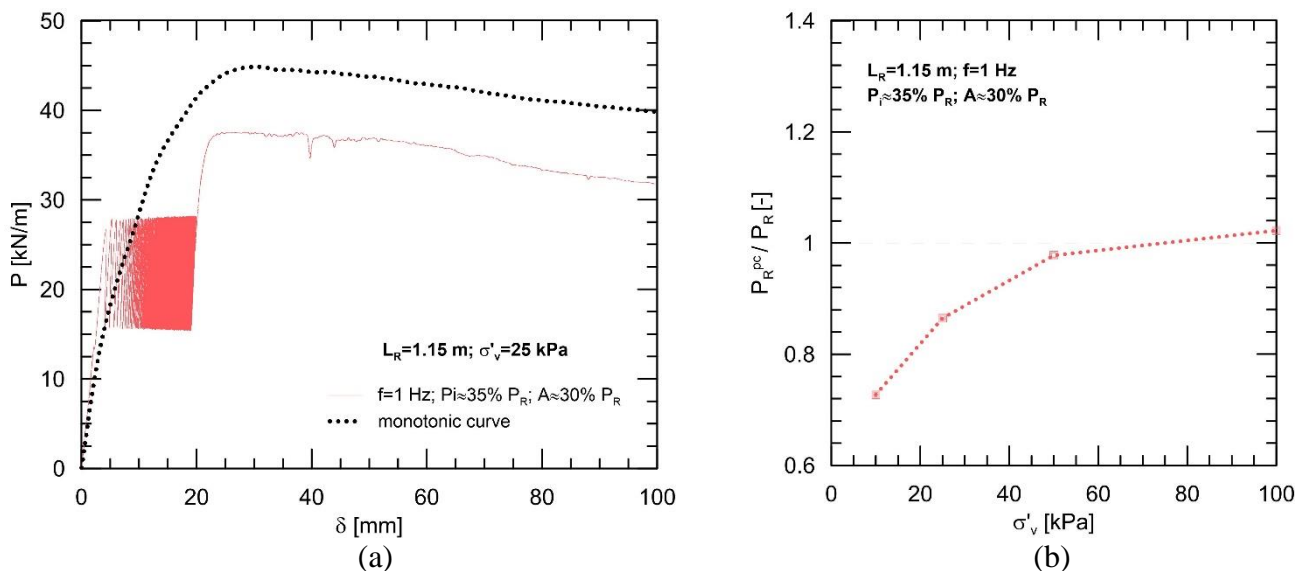


Figure 4. Typical pullout curves obtained in monotonic and multi-stage conditions at $\sigma'_v = 25$ kPa (a) and normalised post-cyclic peak pullout resistance for varying vertical effective stresses (b) at $A \approx 30\% P_R$.

4 CONCLUSIONS

The paper deals with pullout tests carried out on an HDPE geogrid embedded in a well-compacted granular soil under monotonic and cyclic loading conditions. Cyclic and post-cyclic conditions were investigated by means of a multistage procedure, applying different cyclic loading histories characterized by a high frequency ($f = 1$ Hz).

The results show that the soil-geogrid interface behaviour is dependent on both the cyclic loading amplitude and vertical effective stress. The stability of soil-geogrid interface during the cyclic phase starts getting worse with increasing cyclic loading amplitude, while it is possible to note that the increasing of the vertical effective stress σ'_v plays a stabilising role.

Moreover, cyclic loading histories could induce a reduction of the interface parameters with decreasing vertical effective stresses. For the specific test conditions, the post-cyclic peak pullout resistance reaches decreases up to 27% at the lower σ'_v investigated, while it remains almost equal to the corresponding monotonic value at the higher σ'_v .

The decreasing of the interface parameters can be explained by the progressive pullout failure mechanisms of the soil-geogrid interface: the load is transferred on a geogrid's portion that increases during the cyclic phase, involving a reduction of the "supply" of pullout resistance during the post-cyclic phase. At

the lower vertical effective stresses, the decrement is higher since the cumulative displacement along the geogrid is higher (as well as the displacement of each transversal bar) due to the soil dilatancy effect.

REFERENCES

- Bergado, D.T., Shivashankar, R., Alfaro, M.C., Chai, J.-C., Balasubramaniam, A.S. 1993. Interaction behaviour of steel grid reinforcements in a clayey sand. *Geotechnique* Vol. 43(4), 589-603.
- Calvarano, L.S., Gioffrè, D., Cardile, G., Moraci, N. 2014. A stress transfer model to predict the pullout resistance of extruded geogrids embedded in compacted granular soils. In proceeding of the 10th International Conference on Geosynthetics, ICG 2014. Berlin, Germany, 21-24 September 2014, Code 110984.
- Cardile, G., Gioffrè, D., Moraci, N., Calvarano, L.S. 2017a. Modelling interference between the geogrid bearing members under pullout loading conditions. *Geotextiles and Geomembranes*, Vol. 45(3), 169-177.
- Cardile, G., Moraci, N., Calvarano, L.S., 2016a. Geogrid pullout behaviour according to the experimental evaluation of the active length. *Geosynthetics International* Vol. 23(2), 194-205.
- Cardile, G., Moraci, N., Pisano, M. 2016b. In-air Tensile Load-strain Behaviour of HDPE Geogrids Under Cyclic Loading. *Procedia Engineering*, Vol. 158, 266-271.
- Cardile, G., Moraci, N., Pisano, M., 2017b. Tensile behaviour of an HDPE geogrid under cyclic loading: experimental results and empirical modelling. *Geosynthetics International* Vol. 24(1), 95-112.
- ISO (2015). 10319: Geosynthetics Wide-width Tensile Test. International Organization for Standardization, Geneva, Switzerland.
- Dyer, M.R., 1985. Observations of the stress distribution in crushed glass with applications to soil reinforcement, Magdalene College. University of Oxford, Michaelmas Term, p. 220. Ph.D. Thesis.
- Jacobs, F., Ziegler, M., Vollmert, L., Ehrenberg, H. 2014. Explicit design of geogrids with a nonlinear interface model. In proceeding of the 10th International Conference on Geosynthetics, ICG 2014. Berlin, Germany, 21-24 September 2014.
- Min, Y., Leshchinsky, D., Ling, H.I., Kaliakin, V.N., 1995. Effects of Sustained and Repeated Tensile Loads on Geogrids Embedded in Sand. *Geotechnical Testing Journal* Vol. 18(2), 204-225.
- Moraci, N., Cardile, G., 2009. Influence of cyclic tensile loading on pullout resistance of geogrids embedded in a compacted granular soil. *Geotextiles and Geomembranes* Vol. 27, 475-487.
- Moraci, N., Cardile, G., 2012. Deformative behaviour of different geogrids embedded in a granular soil under monotonic and cyclic pullout loads. *Geotextiles and Geomembranes* Vol. 32, 104-110.
- Moraci, N., Cardile, G., Pisano, M. 2017. Soil-geosynthetic interface behaviour in the anchorage zone [Comportamento all'interfaccia terreno-geosintetico nella zona di ancoraggio]. *Rivista italiana di geotecnica*, 51(1), 5-25.
- Moraci, N., Recalcati, P., 2006. Factors affecting the pullout behaviour of extruded geogrids embedded in compacted granular soil. *Geotextiles and Geomembranes* Vol. 24(4), 220-242.
- Nayeri, A., Fakharian, K., 2009. Study on Pullout Behavior of Uniaxial HDPE Geogrids Under Monotonic and Cyclic Loads. *International Journal of Civil Engineering* Vol. 7(4), 211-223.
- Nernheim, A., 2005. Interaktionsverhalten von Geokunststoff und Erdstoff bei statischen und zyklischen Beanspruchungen. TU Clausthal. Ph.D. Thesis.
- Palmeira, E.M., 2009. Soil-geosynthetic interaction: Modelling and analysis. *Geotextiles and Geomembranes*, Vol. 27, 368-390.
- Raju, D.J., Fannin, J., 1997. Monotonic and cyclic pull-out resistance of geogrids. *Geotechnique* Vol. 47(2), 331-337.
- Yasuda, S., Nagase, H., Marui, H., 1992. Cyclic pull-out test of geogrids in soils, International Symposium on Earth Reinforcement Practice, Fukuoka, Japan pp. 185-190.
- Zhou, J., Chen, J.-F., Xue, J.-F., Wang, J.-Q. 2012. Micro-mechanism of the interaction between sand and geogrid transverse ribs. *Geosynthetics International*, Vol. 19(6), 426-437.
- Ziegler, M. & Timmers, V. 2004. A new approach to design geogrid reinforcement. In proceeding of the 3rd European Geosynthetics Conference. Munich, Germany, 01-03 March.